inter.noise
27-30 AUGUST HONG KONG 2017

Effects of the finite circular baffle size on the sound power measurement

Jiaxin ZHONG[1]; Jiancheng TAO[2]; Xiaojun QIU[3]

[1] Key Laboratory of Modern Acoustics and Institute of Acoustics, Nanjing University, China

[2] Key Laboratory of Modern Acoustics and Institute of Acoustics, Nanjing University, China

[3] Centre for Audio, Acoustics and Vibration, Faculty of Engineering and IT, University of Technology Sydney, Australia

ABSTRACT

Sound power measurements are often required in noise control. According to ISO 3745, the reflecting plane shall exceed at least 1/4 wavelength and no less than 0.75 m beyond the measurement surface when the sound power level is measured with microphones at a hemispherical surface in an anechoic chamber. However, the effect of the baffle size on the measured sound power level is still not clear. This paper develops an analytical model to calculate the scattering sound from a monopole noise source above a finite circular baffle. The measurement accuracy by using 10 microphones on a hemispherical surface centered at the baffle center is analyzed based on the scattering model in the spheroidal oblate coordinate system. The correction terms due to the baffle scattering are given for the monopole source at different heights. Numerical simulations are also conducted to validate the proposed model and the specified correction terms.

Keywords: Sound power measurements, Acoustic scattering I-INCE Classification of Subjects Number(s): 72

1. INTRODUCTION

In noise control, sound power level (SWL) plays an important role in characterizing the noise source. SWL is normally determined based on the sound pressure measurements using microphones because the sound intensity sensors are more expensive (1). According to ISO 3745, 10 or 20 or more prescribed microphone positions is chosen on a spherical measurement surface around the noise source under investigation in anechoic rooms or a hemispherical measurement surface in which case the source is mounted above a reflecting plane (2). The reflecting plane laid in anechoic rooms shall exceed at least 1/4 wavelength and no less than 0.75 m beyond the projection of the measurement surface.

In a free field, the inverse square law of sound propagation holds, hence the SWL can be calculated by spatially averaged sound pressure level (SPL) and appropriate correction terms due to meteorological conditions under test. The existence of reflecting plane affects the measurement results but the detailed effect is not mentioned in ISO 3745 because it is difficult to calculate the scattered sound from the reflecting plane. This paper is going to provide an exact solution of the scattering sound when the baffle is circular.

Mathematically, the acoustic scattering due to the circular baffle can be calculated by solving the Helmholtz equation in an unbounded domain with a rigid boundary condition. This problem can be analytically solved in oblate spheroidal coordinates by compressing the oblate spheroid to a disk (3). The spheroidal wave functions (SWFs) used in the solution is difficult to compute (4-6), therefore only far-field solutions are typically calculated based on the asymptotic forms of SWFs (7). In 2014, a

[1] jxzh@smail.nju.edu.cn
[2] jctao@nju.edu.cn
[3] xiaojun.qiu@uts.edu.au

software based on MATLAB is developed to compute the exact solution for the problem over a wide range frequencies and distances (8) and the key of this software is computing the SWFs using arbitrary precision arithmetic (9). After the software is reported, many problems involving spheroids or disks are proposed and solved (10). However, these studies have not been applied to investigate the SWL determination error caused by a finite circle baffle.

The sound scattering model is presented first and then an analytical solution is derived. In Section 3, the error of sound power determination according to ISO 3745 is discussed, and the correction term due to the baffle reflecting is also investigated. Finally, the conclusions of the work are summarized.

2. THEORY

2.1 Sound power level determination

The sound power measurements in anechoic chambers can be conducted using a spherical measurement surface, or using a hemispherical measurement surface together with a reflecting surface. The SWL, L_w, in both methods is calculated by (2)

$$L_W = \overline{L_p} + 10\lg\left(\frac{S_1}{S_0}\right) + C \tag{1}$$

where $\overline{L_p}$ is spatially averaged SPL, S_1 is the area of the measurement surface, S_0 = 1 m^2 is reference area, C is the correction term due to meteorological conditions.

If the reflecting surface is sufficiently large, the total radiation power, W, is (11)

$$W = 2W_0\left(1 + \frac{\sin kH}{kH}\right) \tag{2}$$

where k is the wavenumber, W_0 is the power of an identical point source radiates in free field and H is the height of the source.

When a point source is closely enough to the ground or reflecting plane, or at low frequency, the term $\sin(kH)/(kH)$ in Eq. (2) is approximately 1. Therefore, $W = 4W_0$, which means the reflecting plane magnifies the radiation of the source and leads a 6 dB increment in SWL.

After taking into account the area changes in Eq. (1) (i.e. 4π and 2π for spherical surface and hemispherical surface respectively), there would be theoretically 3 dB error in SWL when a identical noise source placed into free field and half-free field. More generally, when the frequency, the height of the source or the size of the baffle changed, the error would vary significantly. Unfortunately, this error is not discussed in ISO 3745.

To eliminate the calculation error of SWL, a correction term due to the baffle scattering shall be given. Then the Eq. (1) is modified as:

$$L_W = \overline{L_p} + 10\lg\left(\frac{S_1}{S_0}\right) + C - C_b \tag{3}$$

where C_b is the correction terms in dB. Because the placed baffle would enhance the radiation of the source and the measured SPL at same field point would be greater, the minus sign preceding C_b is chosen to let C_b be positive in most frequency bands.

The investigation model is shown in Figure 1, where a monopole source is placed above a circular baffle. The radius of the baffle is a and the height of the source is H. The sound pressure on the upper half space needs to be calculated to determine the SWL according to ISO 3745.

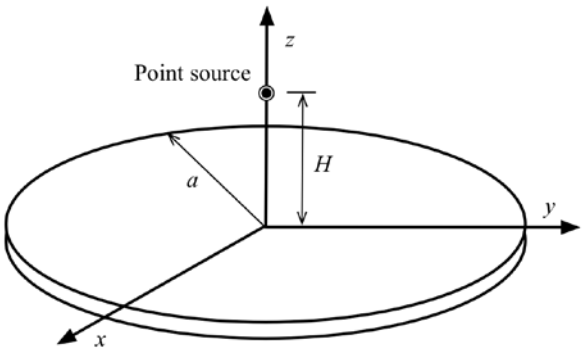

Figure 1 – Sketch of the investigation model

2.2 Acoustic field calculation in oblate spheroidal coordinates

To solve the scattering sound pressure analytically, the oblate spheroidal coordinate system is employed as shown in Figure 2, where φ is the revolutional coordinate about z axis, η and ξ are the spheroidal angular and the radial coordinates respectively. The Cartesian coordinates (x, y, z) in Figure 1 can be presented using oblate spheroidal coordinates as (5)

$$\begin{cases} x = a\left[\left(1-\eta^2\right)\left(1+\xi^2\right)\right]^{1/2}\cos\varphi \\ y = a\left[\left(1-\eta^2\right)\left(1+\xi^2\right)\right]^{1/2}\sin\varphi, \quad \xi\in[0,\infty), \eta\in[-1,1], \varphi\in[0,2\pi). \\ z = a\eta\xi \end{cases} \tag{4}$$

where constant a is the hemi-interfocal distance of the generating ellipses. At far-field ($\xi \to \infty$), the angular coordinate, η, which represents the surface of a hyperboloid, is given by (5)

$$\eta = \cos\theta \tag{2}$$

where θ is the angle between the positive z axis and the asymptote of the hyperboloid. The $\eta = +1$ and $\eta = -1$ represent positive and negative z axis, respectively.

It is clear that when ξ is set as 0, the oblate spheroid degenerates into a circular disk with a radius of a in plane $z = 0$.

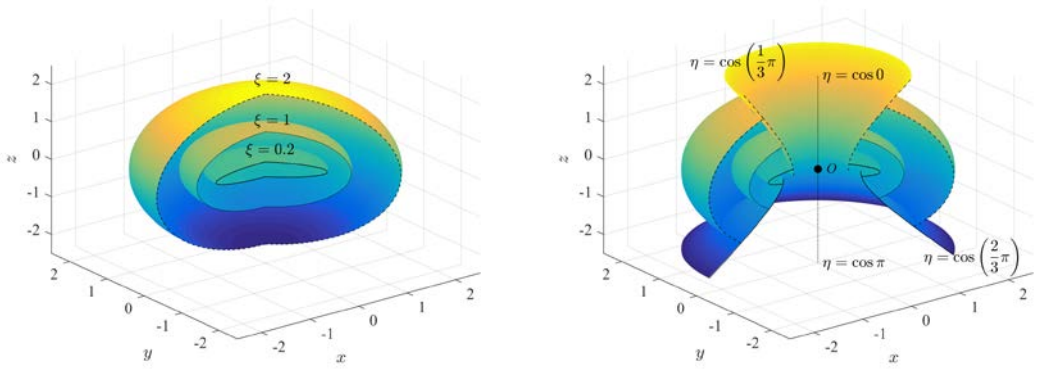

(a) (b)

Figure 2 – The oblate spheroidal coordinates (a) Varying radial coordinate ξ (b) Varying angular coordinate η

Consider Eq. (1), the governing equation of the free field sound wave propagation in oblate coordinates can be written as (5)

$$\left\{\frac{\partial}{\partial\eta}\left[\left(1-\eta^2\right)\frac{\partial}{\partial\eta}\right]+\frac{\partial}{\partial\xi}\left[\left(\xi^2+1\right)\frac{\partial}{\partial\xi}\right]+\frac{\xi^2+\eta^2}{\left(1-\eta^2\right)\left(\xi^2+1\right)}\frac{\partial^2}{\partial\varphi^2}+h^2\left(\xi^2+\eta^2\right)\right\}p=0, \tag{5}$$

where p is the sound pressured and $h = ka$ is the reduced frequency. The general modal solution to the equation is (5)

$$p_{mn}=S_{mn}\left(-\mathrm{j}h,\eta\right)R_{mn}\left(-\mathrm{j}h,\mathrm{j}\xi\right)\begin{Bmatrix}\cos m\varphi\\ \sin m\varphi\end{Bmatrix} \tag{6}$$

where $m = 0, 1, \ldots$ and $n = m, m+1, \ldots$, $S_{mn}(-\mathrm{j}h,\eta)$ and $R_{mn}(-\mathrm{j}h,\mathrm{j}\xi)$ are called oblate spheroidal angular functions (OSAFs) and oblate spheroidal radial functions (OSRFs) respectively. The detail of OSAFs and OSRFs and their computation can refer to references (5) and (6). In the following derivation, the parameter $-\mathrm{j}h$ will be omitted in OSAFs and OSRFs for simplicity presentation.

The incident sound field from the monopole source can be calculated as (11)

$$p_{\mathrm{inc}}\left(\mathbf{r};\mathbf{r}_{\mathrm{ps}}\right)=A\frac{\mathrm{e}^{\mathrm{j}k\left|\mathbf{r}-\mathbf{r}_{\mathrm{ps}}\right|}}{\left|\mathbf{r}-\mathbf{r}_{\mathrm{ps}}\right|} \tag{7}$$

where A is radiation amplitude, $\mathbf{r}$ and $\mathbf{r}_{\mathrm{ps}}$ are the locations of the field point and the sound source respectively. The equation can be expanded in oblate spheroidal coordinates as (5)

$$p_{\mathrm{inc}}\left(\eta,\xi,\varphi;\eta_{\mathrm{ps}},\xi_{\mathrm{ps}},0\right)=2\mathrm{j}kA\sum_{m=0}^{\infty}\sum_{n=m}^{\infty}\frac{2-\delta_{0m}}{N_{mn}}S_{mn}^{(1)}\left(\eta\right)S_{mn}^{(1)}\left(\eta_{\mathrm{ps}}\right)R_{mn}^{(1)}\left(\mathrm{j}\xi_{<}\right)R_{mn}^{(3)}\left(\mathrm{j}\xi_{>}\right)\cos m\varphi \tag{8}$$

where $(\eta_{\mathrm{ps}}, \xi_{\mathrm{ps}}, 0)$ and (η, ξ, φ) are the positions of the point source and field point respectively ($\varphi_{\mathrm{ps}} = 0$ for the symmetry), ρ is the fluid mass density of the medium, c is the sound speed in the medium, $\delta_{ij} = 1$ (only if $i = j$) is the Kronecker Delta function, $\xi_{<} = \min(\xi, \xi_{\mathrm{ps}})$ and $\xi_{>} = \max(\xi, \xi_{\mathrm{ps}})$. The first kind OSAF, $S_{mn}^{(1)}(\eta)$, are orthogonal on the interval $(-1,1)$ and has the normalization integral $N_{mn}(h)$, which is satisfied with (5)

$$\int_{-1}^{1}S_{mn}\left(-\mathrm{j}h,\eta\right)S_{mn'}\left(-\mathrm{j}h,\eta\right)\mathrm{d}\eta=\delta_{nn'}N_{mn}\left(h\right) \tag{9}$$

The first and second kind of OSRFs are $R_{mn}^{(1)}(-\mathrm{j}h,\mathrm{j}\xi)$ and $R_{mn}^{(2)}(-\mathrm{j}h,\mathrm{j}\xi)$ respectively. Another useful combination of these functions is known as functions of the third kind, $R_{mn}^{(3)}(-\mathrm{j}h,\mathrm{j}\xi)$, which represents diverging wave and is therefore related to the standing wave functions by (5)

$$R_{mn}^{(3)}\left(-\mathrm{j}h,\mathrm{j}\xi\right)=R_{mn}^{(1)}\left(-\mathrm{j}h,\mathrm{j}\xi\right)+\mathrm{j}R_{mn}^{(2)}\left(-\mathrm{j}h,\mathrm{j}\xi\right) \tag{10}$$

The scattered sound field is due to the existence of the disk can also be expanded as

$$p_{\mathrm{scat}}=\sum_{m=0}^{\infty}\sum_{n=m}^{\infty}A_{mn}S_{mn}\left(\eta\right)R_{mn}^{(3)}\left(\mathrm{j}\xi\right)\cos m\varphi. \tag{11}$$

Consider the rigid boundary condition

$$\left.\frac{\partial p_{\mathrm{tot}}}{\partial\xi}\right|_{\xi=0}=\left.\frac{\partial\left(p_{\mathrm{inc}}+p_{\mathrm{scat}}\right)}{\partial\xi}\right|_{\xi=0}=0 \tag{12}$$

and the degeneration condition $\xi = 0$ for a disk, the exact analytic solution may be expressed as (5)

$$\begin{aligned}p_{\mathrm{tot}}\left(\eta,\xi,\varphi;\eta_{\mathrm{ps}},\xi_{\mathrm{ps}},\varphi_{\mathrm{ps}}\right)=&\,2\mathrm{j}kA\sum_{m=0}^{\infty}\sum_{n=m}^{\infty}\frac{2-\delta_{0m}}{N_{mn}}S_{mn}^{(1)}\left(\eta\right)S_{mn}^{(1)}\left(\eta_{\mathrm{ps}}\right)\cos m\varphi\\&\times\left[R_{mn}^{(1)}\left(\mathrm{j}\xi_{<}\right)R_{mn}^{(3)}\left(\mathrm{j}\xi_{>}\right)-\frac{R_{mn}^{(1)\prime}\left(0\right)}{R_{mn}^{(3)\prime}\left(0\right)}R_{mn}^{(3)}\left(\mathrm{j}\xi\right)R_{mn}^{(3)}\left(\mathrm{j}\xi_{\mathrm{ps}}\right)\right]\end{aligned} \tag{13}$$

where the prime on the radial functions denotes differentiation with respect to radial coordinate ξ. So far, one can calculate the total acoustic field as soon as the source is given.

When the monopole sound source locates above the disk center as shown in Figure 1, $\eta_{\mathrm{ps}} = 1$ and the terms with $m > 0$ in Eq. (13) can be eliminated (i.e. $S_{m>0,\,n}^{(1)} = 0$) for the symmetry. Hence, the equation reduces to

$$p_{\mathrm{tot}} = 2\mathrm{j}kA\sum_{n=0}^{\infty}\frac{1}{N_{0n}}S_{0n}^{(1)}(\eta)S_{0n}^{(1)}(1)\left[R_{0n}^{(1)}(\mathrm{j}\xi_{<})R_{0n}^{(3)}(\mathrm{j}\xi_{>})-\frac{R_{0n}^{(1)\prime}(0)}{R_{0n}^{(3)\prime}(0)}R_{0n}^{(3)}(\mathrm{j}\xi)R_{0n}^{(3)}(\mathrm{j}\xi_{\mathrm{ps}})\right] \tag{14}$$

According to Eq. (14), we can calculate the sound field numerically at arbitrary field point by adding the first few terms of the series.

3. RESULTS AND DISCUSSION

3.1 Numerical simulations

Numerical simulations by Virtual Lab Acoustics were conducted to validate the proposed model and the given correction terms. Virtual Lab Acoustics is a kind of software that can calculate acoustic noise with high precision. For the scattering problem investigated in this paper, the boundary element model (BEM) is used. All the physical parameters of the model considered is the same in Section 3.2 and Section 3.3. The maximum reduced frequency *ka* is chosen to 18 for the sake of the limiting size of the BEM model computed in software.

Figure 3 shows comparisons between theoretical results and numerical simulations ones. As we can see from the figure, in the interested bands of frequency, the results computed by the theory agree with the numerical simulations satisfactorily and the maximum level difference is less than 0.2 dB. This assures that the numerical solution of theory converges to the correct one.

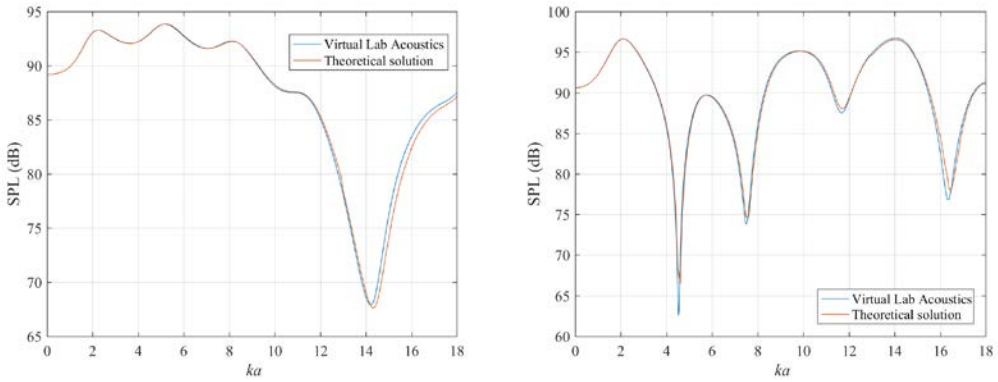

(a) (b)

Figure 3 – Sound pressure level at several field points specified in ISO 3745 when H = 0.25 m and a = 1 m (a) Field point (−0.675, 1.155, 0.675) m (b) Field point (0.495, −0.855, 1.125) m

3.2 Deviation on hemispherical measurement surface

Figure 4 shows the sound field due to a monopole source located 0.01 m above the disk center. The largest value of h here is set to 15, below which its numerical results are validated compared by numerical simulations as discussed in Section 3.1. For higher reduced frequency h, the computation of SWFs requires precision beyond the double floating point numbers in commercial computers (12). In this case, one may implement a specialized C++ Library called GNU MPFR Library to use arbitrary precision arithmetic (13, 14).

When h is sufficient small ($h \leq 1$), the baffle has little effect on the directivity of the source. Therefore, the SPL on a hemispherical measurement surface is uniform and the Eq. (1) can be applied to calculate the SWL of the noise source with 3 dB correction.

As the reduced frequency or the radius of the measurement surface increases, deviations occur on a hemispherical measurement surface. In the example illustrated in Figure 4, there would be more than 15 dB deviation on the measurement surface when the surface radius is 1.5 m and h = 15. However, as described in Annex A of ISO 3745, the maximum allowable deviation of measured sound pressure levels from theoretical levels shall be less than 3 dB in all the 1/3-octave bands. Consequently, in most real situations, these specifications cannot meet and there would be a large error when calculate the SWL using formulas proposed in ISO 3745.

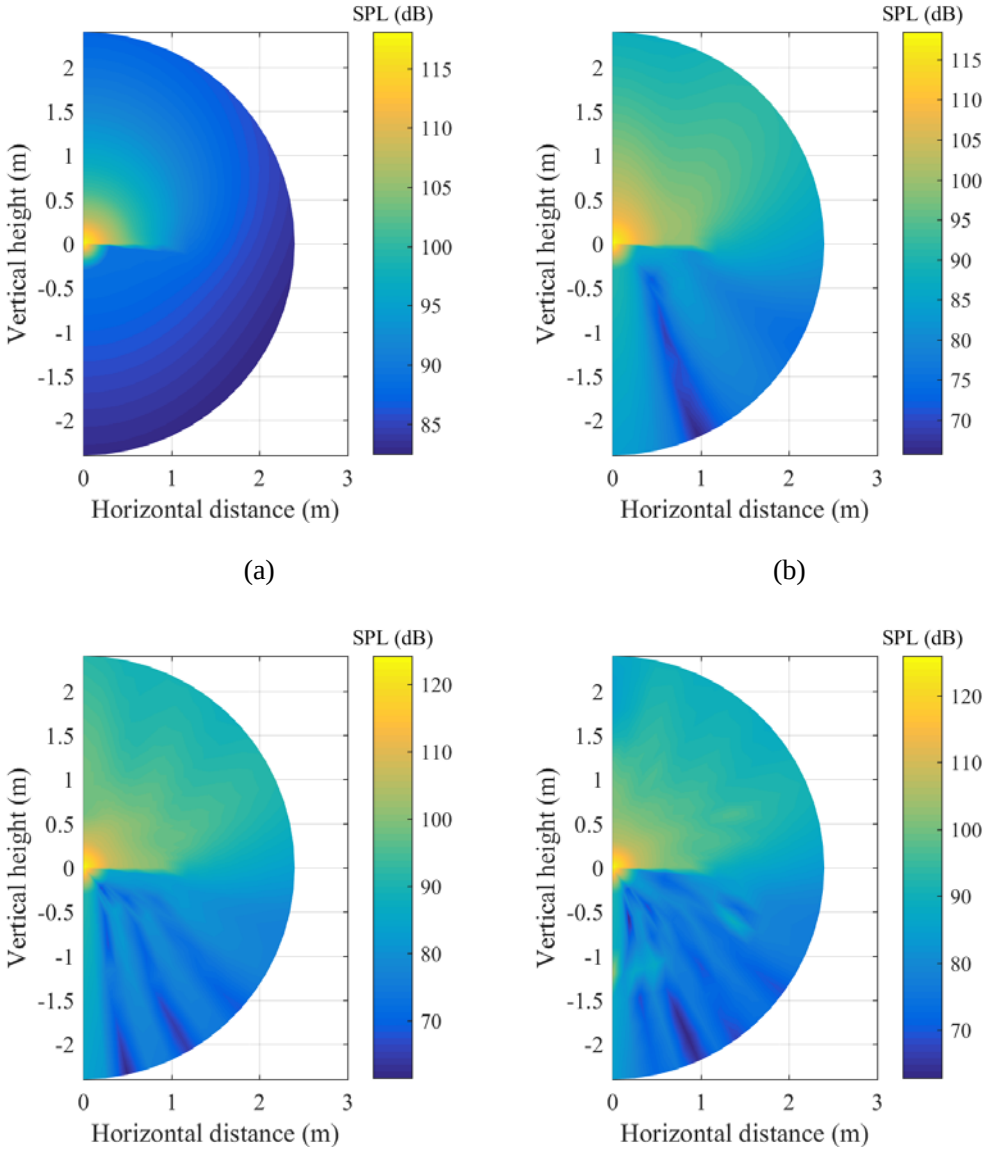

Figure 4 – Computed sound field for a monopole source at the center axis when H = 0.01 m and a = 1 m

(a) h = 1 (b) h = 6 (c) h = 12 (d) h = 15

3.3 Correction terms of measurement

As mentioned in Section 2.1 and Section 3.2, the calculation error in Eq. (1) is discernible and non-negligible. It is obviously that the values of correction terms relate to frequency. Because 1/3-octave analysis is often used in noise control field, the correction terms for the monopole source with a constant radiation amplitude at different heights, are computed and listed in Table 1.

Table 1 shows that the values of correction terms depend on the height of the source and fluctuate in frequency. In a particular case, when H = 0.01 m, with the frequency increasing, C_b is approximately 3 dB. This is because $ka \gg 1$, the disk can be regarded as a infinite baffle, and $kH \ll 1$, the low frequency approximation in Eq. (2) holds. Consequently, a 3 dB increment occurs as expected.

Table 1 – Values of correction terms, C_b, for mid-band frequencies of one-third-octave bands (a = 0.5 m)

1/3-octave mid-band frequency	Correction terms C_b (dB) with different heights of source				
(Hz)	H = 0.01 m	H = 0.1 m	H = 0.2 m	H = 0.4 m	H = 0.5 m
50	−1.8	−1.8	−1.8	−1.7	−1.6
63	−1.7	−1.7	−1.6	−1.6	−1.5
80	−1.5	−1.5	−1.5	−1.4	−1.3
100	−1.2	−1.2	−1.2	−1.1	−1.0
125	−0.5	−0.5	−0.5	−0.5	−0.4
160	0.8	0.8	0.8	0.8	0.7
200	2.6	2.6	2.5	2.2	1.9
250	3.7	3.6	3.4	2.5	1.8
315	3.1	3.0	2.5	0.7	−0.7
400	2.3	2.0	1.2	−1.5	−3.0
500	2.4	2.0	1.1	−1.1	−1.0
613	3.2	2.7	1.4	−1.2	−1.1
800	2.9	2.1	−0.4	−2.0	−0.4
1000	3.2	1.9	−1.1	0.5	0.1
1250	2.4	0.9	0.1	0.5	−0.7
1600	3.3	0.7	0.2	−2.6	−0.4
2000	3.7	−0.4	−1.2	0.6	0.3
2500	2.4	−2.2	0.3	−0.7	−2.1

4. CONCLUSIONS

In this paper, the measurement error due to a reflecting plane of sound power measurements according to ISO 3745 is investigated and the corresponding correction terms are given analytically. The results show that for a monopole source, the SWL determined according to ISO 3745 is more than 3 dB larger than the actual value at some frequencies, and it needs to be corrected depending on the frequency. When the source is sufficiently close to the reflecting plane (i.e. $kH \ll 1$) and the size of the reflecting plane is non-negligible (i.e. $ka \gg 1$), the SWL correction term converges to be 3 dB.

ACKNOWLEDGEMENTS

This research was supported under the Australian Research Council's Linkage Projects funding scheme (LP140100987) and by the National Science Foundation of China (11474163).

REFERENCES

1. Petersen, Cletus E. An overview of standards for sound power determination. Brüel & Kjær; 1994.
2. ISO. Acoustics - Determination of Sound Power Levels and Sound Energy Levels of Noise Sources Using Sound Pressure - Precision Methods for Anechoic Rooms and Hemi-anechoic Rooms (ISO 3745:2012(E)). International Organization for Standardization; 2012.
3. Spence RD. The diffraction of sound by circular disks and apertures. J Acoust Soc Am. 1948;20(4):380-6.
4. Stratton JA, Morse PM, Chu LJ, Hutner RA. Elliptic Cylinder and Spheroidal Wave Functions: Including Tables of Separation Constants and Coefficients. New York, USA: John Wiley & Sons, inc.;

1941.
5. Flammer C. Spheroidal Wave Functions. Mineola, New York, USA: Dover Publications, Inc.; 1957.
6. Zhang S, Jin J. Computation of Special Functions. New York, USA: John Wiley & Sons, Inc.; 1996.
7. Lauchle GC. Radiation of sound from a small loudspeaker located in a circular baffle. J Acoust Soc Am. 1975;57(3):543-9.
8. Adelman R, Gumerov NA, Duraiswami R. Semi-analytical computation of acoustic scattering by spheroids and disks. J Acoust Soc Am. 2014;136(6):El405-El10.
9. Adelman R, Gumerov NA, Duraiswami R. Software for computing the spheroidal wave functions using arbitrary precision arithmetic. arXiv preprint arXiv:14080074. 2014.
10. Gonzalez JD, Lavia EF, Blanc S. A computational method to calculate the exact solution for acoustic scattering by fluid spheroids. Acta Acust United Ac. 2016;102(6):1061-71.
11. Morse PM, Ingard KU, Stumpf FB. Theoretical Acoustics. New York, USA: McGraw-Hill; 1968.
12. Van Buren AL, Boisvert JE. Accurate calculation of prolate spheroidal radial functions of the first kind and their first derivatives. Q Appl Math. 2002;60(3):589-99.
13. Foussel L, Hanrot G, Vincent L, Patrick P, Loria PZ. MPFR: A multiple-precision binary floating-point library with correct rounding. Acm T Math Software. 2007;33(2).
14. The GNU MPFR Library: INRIA; [Available from: http://www.mpfr.org/].